Supporting Information

Voityuk et al. 10.1073/pnas.1402025111

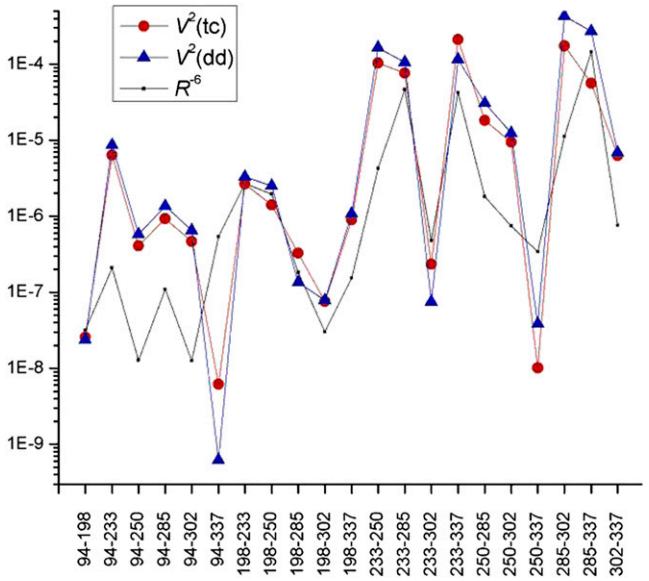

Fig. S1. Excitonic coupling squared (eV^2) computed with the dipole–dipole and transition charge models for L_a excited states of Trp residues.

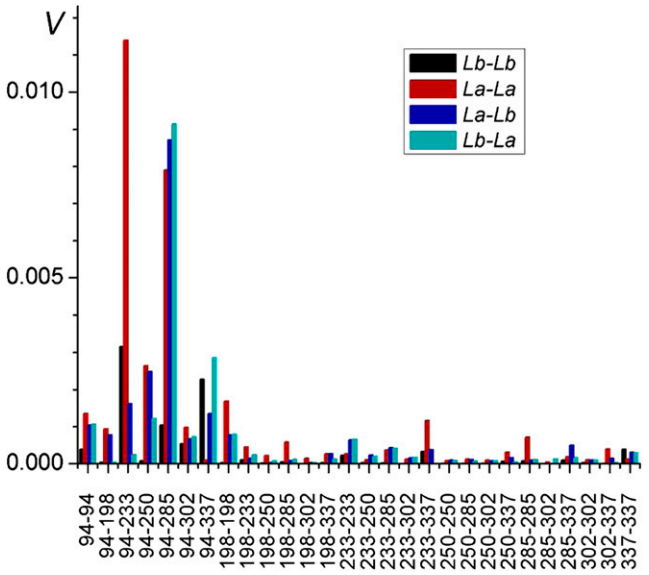

Fig. S2. Intersubunit excitonic coupling (eV) of L_a and L_b excited states of Trp residues.

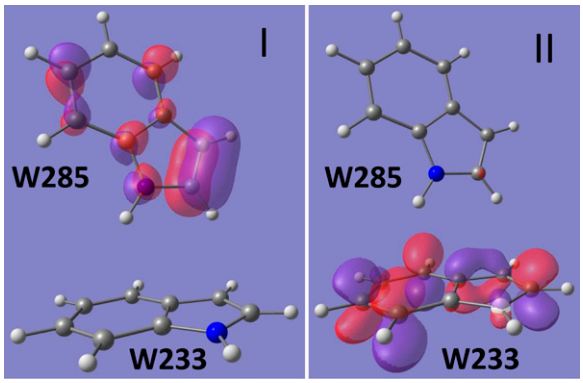

Fig. S3. Formation of the charge transfer (CT) state [$W233^{-}$ $W285^{+}$] by electron transfer from the initial occupied orbital of W285 (I) to the vacant orbital of W233 (II).

Table S1. Relative stabilization energy of L_a states of Trps in the unit A by electrostatic interaction with amino acid residues of the A and B subunits (all energies are in eV)

Trp	A	A + B	Most important residues of A	Most important residues of B
W233	−1.01	−0.66	D129 −0.51, R234 −0.28	D96 +0.26
W285	−0.66	−0.15	D129 −0.16, R234 +0.15, R338 −0.23	D44 +0.21, D107 +0.21
W337	−0.12	+0.19	R44 −0.12	D44 +0.13
W94	−0.76	−0.13	D96 −0.34, D107 −0.33	R286 +0.27
W198	−0.49	−0.39	E182 −0.30	R146 +0.22
W250	−0.60	−0.26	D263 −0.33	D96 +0.28
W302	−0.57	−0.24	D315 −0.38, R286 −0.20, R338 −0.19	E43 +0.11, D44 +0.12

As can be seen, the electrostatic potential of A residues stabilizes the L_a states of Trps. Taking into account both units, A + B, leads to smaller stabilization energies because B residues destabilize the L_a states. We note that the L_b excitation energy of Trps remains almost unchanged (in most cases the effect is smaller than 0.05 eV).

Table S2. Average separation (Å) and EET couplings (eV) of Trp residues in UVR8 (subunit A)

Chromophores	*R*, Å	$V(L_b\text{-}L_b)$	$V(L_a\text{-}L_a)$	$V(L_b\text{-}L_a)$	$V(L_a\text{-}L_b)$
W94-W198	12.96	0.367E-04	0.928E-03	0.792E-03	0.372E-04
W94-W233	6.85	0.313E-02	0.112E-01	0.155E-02	0.225E-03
W94-W250	10.99	0.349E-04	0.293E-02	0.233E-02	0.115E-02
W94-W285	5.90	0.128E-02	0.729E-02	0.865E-02	0.921E-02
W94-W302	10.66	0.492E-03	0.115E-02	0.633E-03	0.777E-03
W94-W337	7.61	0.217E-02	0.846E-04	0.145E-02	0.285E-02
W198-W233	8.46	0.283E-03	0.162E-02	0.207E-02	0.248E-02
W198-W250	8.94	0.307E-03	0.119E-02	0.207E-02	0.507E-03
W198-W285	13.28	0.951E-04	0.573E-03	0.712E-03	0.327E-03
W198-W302	17.92	0.578E-04	0.276E-03	0.268E-03	0.186E-04
W198-W337	13.66	0.846E-04	0.947E-03	0.264E-03	0.396E-03
W233-W250	7.86	0.877E-03	0.102E-01	0.286E-02	0.131E-02
W233-W285	5.28	0.639E-02	0.869E-02	0.229E-02	0.927E-02
W233-W302	11.30	0.271E-03	0.483E-03	0.424E-03	0.788E-03
W233-W337	5.36	0.291E-02	0.145E-01	0.108E-01	0.668E-02
W250-W285	9.06	0.517E-03	0.428E-02	0.138E-02	0.971E-03
W250-W302	10.50	0.182E-03	0.306E-02	0.294E-03	0.122E-03
W250-W337	11.96	0.121E-03	0.101E-03	0.360E-04	0.916E-03
W285-W302	6.69	0.182E-02	0.132E-01	0.405E-02	0.844E-03
W285-W337	4.36	0.551E-02	0.746E-02	0.101E-01	0.208E-02
W302-W337	10.47	0.834E-04	0.250E-02	0.160E-02	0.164E-02

Table S3. Electrostatic potential changes on proton donor and acceptor atoms due to charge separation in the triad W233-W285-W337

Salt bridge	H bond	$R_{N\text{-}O}$, Å	$\Delta\varphi(N)-\Delta\varphi(O)$, eV
R286-D107	N1-O2	2.67	0.325
	N2-O1	3.100	0.425
R286-D96	N2-O2	3.02	1.199
R338-D44	N2-O1	2.95	0.341
R354-E53	N1-O2	2.94	0.068
E182-R146	O1-N1	2.96	0.146
	O2-N2	2.76	0.101